

# Discovering Process–Outcome Credit in Multi-Step LLM Reasoning

Xiangwei Wang<sup>1</sup> Wei Wang<sup>1</sup> Ken Chen<sup>1</sup> Nanduni Nimal Siri<sup>2</sup> Saman Halgamuge<sup>1</sup>

## Abstract

Reinforcement Learning (RL) serves as a potent paradigm for enhancing reasoning capabilities in Large Language Models (LLMs), yet standard outcome-based approaches often suffer from reward sparsity and inefficient credit assignment. In this paper, we propose a novel framework designed to provide continuous reward signals, which introduces a Step-wise Marginal Information Gain (MIG) mechanism that quantifies the intrinsic value of reasoning steps against a Monotonic Historical Watermark, effectively filtering out training noise. To ensure disentangled credit distribution, we implement a Decoupled Masking Strategy, applying process-oriented rewards specifically to the chain-of-thought (CoT) and outcome-oriented rewards to the full completion. Additionally, we incorporate a Dual-Gated SFT objective to stabilize training with high-quality structural and factual signals. Extensive experiments across textual and multi-modal benchmarks (e.g., MATH, Super-CLEVR) demonstrate that our approach consistently outperforms baselines such as GRPO in both sample efficiency and final accuracy. Furthermore, our model exhibits superior out-of-distribution robustness, demonstrating promising zero-shot transfer capabilities to unseen and challenging reasoning tasks.

## 1. Introduction

While Supervised Fine-Tuning (SFT) has long been the primary paradigm for cultivating reasoning in Large Language Models (LLMs), it is fundamentally constrained by its reliance on expert data and a tendency toward surface-level memorization (Zhang et al., 2024; Su et al., 2025). To overcome these limitations, the Reinforcement Learning with Verifiable Rewards (RLVR) framework, popularized by DeepSeek-R1-Zero (DeepSeek-AI et al., 2025), formalizes the reasoning task as a reinforcement learning problem

<sup>1</sup>The University of Melbourne <sup>2</sup>CSIRO. Correspondence to: Xiangwei Wang <xiangwei.wang@student.unimelb.edu.au>.

Preprint. February 3, 2026.

characterized by sparse, objective rewards. In this framework, the LLM policy is optimized to produce a sequence of reasoning steps followed by a terminal answer. A key merit of RLVR is its reliance on a rule-based evaluator that assigns a binary reward signal  $\{0, 1\}$  based on the correctness of the final response. This approach enables the model to explore and refine its internal reasoning logic without requiring dense human feedback (Yue et al., 2025).

Despite the promise of RLVR, the efficacy of outcome-only rewards is fundamentally limited by reward sparsity, particularly in complex reasoning chains where the binary feedback provides no signal for intermediate correctness. To alleviate this, dense rewards are often introduced; however, existing paradigms face a dual bottleneck. On one hand, Process Reward Models (PRMs) (Zhang et al., 2025c) rely on labor-intensive, human-annotated rationales, which pose a significant barrier to autonomous scaling. On the other hand, alternative dense signals—often derived from hand-crafted rules or auxiliary models—are frequently susceptible to reward hacking (Sahoo, 2025; Zhang et al., 2025a). Crucially, these surrogates often exhibit a semantic disconnect, struggling to accurately quantify the functional proximity between intermediate reasoning steps and the terminal goal.

These challenges motivate a fundamental question: *How can we architect a learning framework that facilitates dense, step-wise semantic guidance while ensuring rigorous outcome alignment, all without resorting to exogenous expert demonstrations?*

To this end, we propose a learning framework that enables LLMs to achieve autonomous reasoning through intrinsic, dense semantic feedback. Our core idea is to move beyond fragile external proxies and instead derive guidance from the model’s internal probabilistic transitions.

Specifically, our contributions are as follows:

- **Process Exploration via Step-wise Probabilistic Reward:** Acknowledging that reasoning is inherently divergent (a *many-to-one* mapping where infinite paths lead to the same truth), we propose a dense reward mechanism that facilitates broad *cognitive exploration* rather than strict imitation. By calculating the Marginal Information Gain (MIG) against a *monotonic historical watermark*, our method encourages the model to dis-

cover diverse, feasible reasoning trajectories within a vast solution space. This effectively resolves the credit assignment problem by rewarding *intrinsic semantic novelty*. Our method isolates the intrinsic semantic novelty of each step regardless of its sequential position. This effectively filters out redundant oscillations and provides a smooth, hard-to-hack gradient signal that resolves the credit assignment problem with content-aware precision.

- **Outcome Grounding via Gated Self-Correction:** In contrast to the divergence of reasoning, the correctness of the final answer is strictly convergent. To enforce this, we introduce an *Outcome-Gated Self-Correction* strategy. This mechanism applies SFT *exclusively* when the model’s exploratory trajectory converges to a verified correct outcome. By treating only successful self-generated paths as positive training samples, we enable high-fidelity data distillation that balances **creative process exploration with strict outcome adherence**, preventing the accumulation of logical hallucinations.
- **Hybrid Reward Optimization with Decoupled Masking:** To synergize divergent exploration and convergent grounding, which are opposing objectives, we design a dual-objective optimization scheme implemented via a **Decoupled Masking Strategy**. This ensures that the dense reward guides the expansion of the reasoning search space, while the sparse binary reward and gated SFT strictly bound the optimization within the manifold of correctness, effectively bridging the gap between open-ended thinking and precise answering.
- **Cross-Modal Scalability and Generalization:** We demonstrate the universality of our framework by extending it beyond text-only domains to complex multi-modal reasoning tasks. Our approach exhibits superior transferability. This substantiates that the intrinsic semantic novelty captured by our reward is a modality-agnostic driver of general intelligence.

## 2. Related Work

**Reinforcement Learning (RL) for LLM Reasoning**  
 RL has emerged as a central paradigm for eliciting the latent reasoning potential of LLMs, demonstrated by the success of systems like OpenAI-o1 (OpenAI et al., 2024), Kimi K2 (Team et al., 2025) and DeepSeek-R1 (DeepSeek-AI et al., 2025). The dominant outcome-based paradigm, pioneered by Group Relative Policy Optimization (GRPO) (Shao et al., 2024), estimates policy gradients via group-relative advantages, efficiently eliminating the need for value networks. Recent advances such

as Decoupled Advantage Policy Optimization (DAPO) (Yu et al., 2025), Generalized Simple Preference Optimization (GSPO) (Zheng et al., 2025), and Generalized Direct Preference Optimization (GDPO) (Liu et al., 2026) further refine this framework by introducing stabilized clipping, sequence-level policy ratios, and decoupled multi-reward normalization to enhance sample efficiency. Nevertheless, outcome-only supervision inherently suffers from reward sparsity, complicating credit assignment in long-horizon reasoning tasks where binary feedback offers no intermediate guidance. To address this, Process Reward Models (PRMs) (Zhang et al., 2025b;a;c) have been proposed to provide dense supervision. However, the development of effective PRMs faces significant bottlenecks, particularly the reliance on expensive human annotation and the fragility of handcrafted heuristics (Sahoo, 2025), which are susceptible to reward hacking. Consequently, a growing body of research explores Verifier-Free approaches that derive intrinsic dense signals from the model’s internal probability space. Methods like VeriFree (Zhou et al., 2025), JEPO (Tang et al., 2025) and LaTRO (Chen et al., 2024a) utilize the conditional probability of the reference answer. While semantically grounded, such approaches typically offer a holistic trace-level signal, lacking the granularity to distinguish specific logical breakthroughs from redundant tokens. In this work, our approach formalizes a **Step-wise Marginal Information Gain (MIG)** framework. Instead of relying on trace-level holism or position-based biases, we evaluate each reasoning step against a **monotonic historical watermark**, solving the credit assignment problem with **content-aware precision**.

**Self-Improvement and Iterative Refinement** Beyond direct optimization, recent paradigms emphasize iterative self-improvement to scale reasoning capabilities. Seminal approaches such as STaR (Zelikman et al., 2022), CARE-STaR (Li et al.), and ReST (Gulcehre et al., 2023) employ a “generate-filter-train” loop, where model-generated trajectories are filtered by ground-truth correctness and utilized as positive samples for Supervised Fine-Tuning (SFT). However, these outcome-driven mechanisms suffer from Process Agnosticism: they cannot distinguish between rigorously deduced solutions and spurious guesses (false positives), nor can they penalize circular or redundant reasoning as long as the final answer is correct. To internalize feedback, methods such as Bootstrapping with DPO (Chen et al., 2025a) and Self-Rewarding LMs (Yuan et al.) utilize model-internal signals to drive alignment. Yet, these approaches typically treat reasoning trajectories as monolithic units, relying on coarse preference judgments. This lack of granularity makes them insufficient for disentangling divergent process exploration from convergent outcome grounding, leaving models vulnerable to reward hacking and accumulated bias. In contrast, our **Outcome-Gated Self-Correction** strategy introduces a dual-verification mechanism. By conditioning data dis-

tillation on both outcome correctness (to ensure validity) and intrinsic semantic breakthroughs via MIG (to ensure efficiency), we guarantee that self-generated training data is not only accurate but also structurally dense, preventing the degeneration of reasoning chains often observed in purely outcome-filtered methods.

### 3. Methodology

The overall architecture of our framework is illustrated in Figure 1, which consists of three phases: (1) Structured Rollout phase to parse model output into discrete reasoning steps; (2) Step-Aware Probe to reward steps bringing marginal information gain; (3) Optimization and update phase to synergize dense intrinsic rewards with sparse outcome signals.

#### 3.1. Preliminaries and Structured Rollout

We consider a reasoning task where a policy  $\pi_\theta$  generates a reasoning chain  $z$  followed by a final answer  $y$ . Following the Group Relative Policy Optimization (GRPO) paradigm (Shao et al., 2024), for each prompt  $x$ , we sample a group of trajectories  $\{z^{(1)}, \dots, z^{(G)}\}$ . To enable fine-grained credit assignment, we parse each trajectory  $z^{(i)}$  into a sequence of  $K$  discrete reasoning steps  $(s_1, s_2, \dots, s_K)$  using a predefined structural schema (e.g., `<think>...## Step i...</think>`). Unlike outcome-only methods that assign a single scalar reward to the entire chain, our goal is to compute a dense reward vector  $\mathbf{r} = (r_1, \dots, r_K)$  reflecting the intrinsic logical contribution of each step.

#### 3.2. Step-wise Marginal Information Gain (MIG)

A core challenge in dense reward shaping is defining a robust signal that measures logical progress. We introduce **Marginal Information Gain (MIG)**, which rewards steps solely based on their contribution to reducing the uncertainty of the ground truth.

**Step-Conditioned Likelihood.** For a reasoning step  $s_k$  at time step  $k$ , we first quantify its semantic alignment with the ground truth  $y^*$  by computing the length-normalized log-likelihood of  $y^*$  conditioned on the prefix generated so far:

$$\ell_k = \frac{1}{|y^*|} \sum_{t=1}^{|y^*|} \log \pi_\theta(y^* | x, s_{1\dots k}, y^*_{<t}) \quad (1)$$

where  $\ell_0$  represents the baseline likelihood given only the prompt  $x$ . This metric  $\ell_k$  serves as a real-time proxy for the model’s confidence in the correct outcome. We discuss and validate the effectiveness of this proxy measure in Appendix B.

**Monotonic Historical Watermark (HWM).** To prevent

reward hacking via “pump-and-dump” oscillations (where a model degrades likelihood only to improve it later), we enforce a strict monotonicity constraint. We define a **Historical Watermark**  $h_k$  that tracks the maximum semantic fidelity achieved up to step  $k$ :

$$h_k = \max(h_{k-1}, \ell_k), \quad \text{with } h_0 = \ell_0 \quad (2)$$

where  $\ell_0$  is the baseline likelihood given only the prompt.

**Rectified Breakthrough Reward.** The dense reward  $g_k$  is quantified as the rectified increment above this watermark:

$$g_k = \max(0, \ell_k - h_{k-1}) \quad (3)$$

This mechanism ensures that rewards are position-agnostic: a pivotal logical breakthrough yields a high  $g_k$  regardless of whether it occurs early or late in the chain, while redundant steps (where  $\ell_k \leq h_{k-1}$ ) receive zero credit.

#### 3.3. Hybrid Optimization via Decoupled Masking

We propose a multi-objective loss function that decouples process exploration from outcome constraints. The total loss  $\mathcal{L}$  is a weighted sum of three components:

$$\mathcal{L} = \alpha \mathcal{L}_{\text{MIG}} + \beta \mathcal{L}_{\text{Outcome}} + \gamma \mathcal{L}_{\text{Gated-SFT}} \quad (4)$$

**Step-wise MIG Loss ( $\mathcal{L}_{\text{MIG}}$ ).** This term optimizes the reasoning process using the dense rewards. We compute the advantage  $A_i^{\text{step}}$  by normalizing the cumulative MIG scores  $\sum g_k$  within the group. This advantage is applied specifically to the reasoning tokens via a CoT mask  $M_{\text{cot}}$ :

$$\mathcal{L}_{\text{MIG}} = -\frac{1}{G} \sum_{i=1}^G \frac{1}{|z^{(i)}|} \sum_{t \in M_{\text{cot}}} \frac{\pi_\theta(z_t^{(i)} | \cdot)}{\pi_{\text{ref}}(z_t^{(i)} | \cdot)} A_i^{\text{step}} \quad (5)$$

**Outcome & Format Loss ( $\mathcal{L}_{\text{Outcome}}$ ).** To enforce both global correctness and structural adherence, we apply a standard GRPO loss on the entire completion. Crucially, the advantage term here is a hybrid signal. We combine the binary correctness reward  $r_{\text{acc}} \in \{0, 1\}$  with a format compliance reward  $r_{\text{fmt}}$  (checking for valid delimiters like `<think>` and `<answer>`). The combined advantage  $A_i^{\text{outcome}}$  is computed as:

$$A_i^{\text{outcome}} = \text{GroupNorm}(r_{\text{fmt}}^{(i)}) + \gamma \cdot \text{GroupNorm}(r_{\text{acc}}^{(i)}) \quad (6)$$

where  $\gamma$  is a balancing coefficient. This advantage propagates through the whole sequence mask  $M_{\text{comp}}$ , reinforcing trajectories that are both **structurally valid** and **factually correct**:

$$\mathcal{L}_{\text{Outcome}} = -\frac{1}{G} \sum_{i=1}^G \frac{1}{|z^{(i)} \cup y^{(i)}|} \sum_{t \in M_{\text{comp}}} \frac{\pi_\theta(t | \cdot)}{\pi_{\text{ref}}(t | \cdot)} A_i^{\text{outcome}} \quad (7)$$

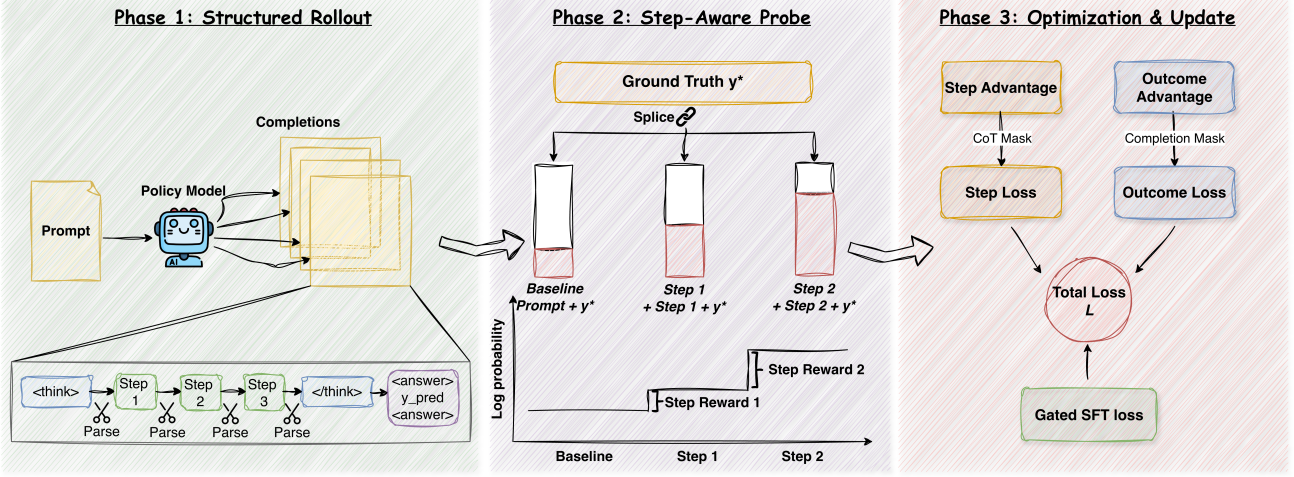


**Figure 1. Overview of the proposed Framework.** Our approach synergizes intrinsic exploration with strict outcome alignment through three key mechanisms: **(Left) Group Sampling:** For each prompt, we sample a group of trajectories and parse them into discrete steps using strict structural tags. The exact prompt template and a concrete case study of the step-wise generation are detailed in Appendix A. **(Middle) Step-wise Marginal Information Gain (MIG):** We calculate the dense reward  $g_k$  as the rectified semantic breakthrough against a *Monotonic Historical Watermark* ( $h_{k-1}$ ), strictly rewarding only non-monotonic logical discoveries. **(Right) Decoupled Hybrid Optimization:** The final objective combines the dense signal (for process exploration) and sparse correctness feedback (for outcome constraint) via a decoupled masking strategy, ensuring that intrinsic curiosity operates strictly within the bounds of correctness.

**Outcome-Gated SFT ( $\mathcal{L}_{\text{Gated-SFT}}$ ).** To stabilize training, we incorporate a self-supervised distillation term. Crucially, this loss utilizes a dual-gating mechanism derived from two weight tensors: (1)  $\omega_{\text{struct}}^{(i)}$ , which indicates if the trajectory follows the valid structural format (i.e., successfully parsed answer tags); and (2)  $\omega_{\text{acc}}^{(i)}$ , which measures the correctness of the answer. The loss is activated only when *both* conditions are met, ensuring high-fidelity data distillation:

$$\mathcal{L}_{\text{Gated-SFT}} = -\frac{1}{G} \sum_{i=1}^G \underbrace{\omega_{\text{struct}}^{(i)} \cdot \omega_{\text{acc}}^{(i)}}_{\text{Dual Gate}} \cdot \log \pi_{\theta}(z^{(i)}, y^{(i)} | x) \quad (8)$$

In our implementation,  $\omega_{\text{struct}}^{(i)} = 1$  if the parser detects valid delimiters, and  $\omega_{\text{acc}}^{(i)} = 1$  if  $y^{(i)} \in \mathcal{Y}^*$ , otherwise they are 0.

By separating these objectives, our framework enables the model to aggressively explore logical paths (driven by  $\mathcal{L}_{\text{MIG}}$ ) without violating the hard constraint of answer correctness (enforced by  $\mathcal{L}_{\text{Outcome}}$  and  $\mathcal{L}_{\text{Gated-SFT}}$ ). Appendix C provides a detailed description of the complete training procedure, as summarized in Algorithm 1.

## 4. Experiments

We conduct extensive experiments to evaluate the effectiveness, robustness, and scalability of our proposed framework, guided by the following three key questions.

1. **Performance:** Does our Step-wise MIG reward outperform traditional GRPO?

2. **Granularity:** Does the Monotonic Historical Watermark (HWM) provide superior credit assignment compared to position-biased or trajectory-level heuristics?
3. **Universality:** Can our intrinsic reward mechanism generalize to multimodal reasoning tasks beyond text?

### 4.1. Experimental Setup

**Training Tasks and Datasets.** To rigorously evaluate our framework across diverse reasoning modalities, we conduct RL training on a suite of eight datasets. We evaluate performance on their respective held-out test sets to measure in-domain mastery:

- **Textual Reasoning:** We utilize **GSM8K** (Cobbe et al., 2021) and **MATH** (Hendrycks et al., 2021) for mathematical deduction, alongside **Tal-SCQ5K-CN** and **Tal-SCQ5K-EN** (Liu et al., 2025a) for scientific reasoning.
- **Multimodal Reasoning:** For vision-language tasks, we train on **CMM-Math** (Liu et al., 2025b) and **ChartQA** (Masry et al., 2022) for real-world visual analysis, and **Super-CLEVR** (Li et al., 2023) alongside **CLEVR-CoGenT** (Chen et al., 2025b) for multi-step synthetic logic.

**Out-of-Distribution (OOD) Benchmarks.** Beyond in-domain evaluations, we assess the generalization capabilities of our model on six external benchmarks. These include

**CommonsenseQA** (Talmor et al., 2019), **SVAMP** (Patel et al., 2021), and **AIME 2025** (Wu et al., 2025) for textual reasoning robustness, as well as **MMStar** (Chen et al., 2024b), **HallusionBench** (Guan et al., 2024), and **Math-Vista** (Lu et al., 2023) for multimodal reasoning transferability.

**Handling Solution Variants.** A critical limitation in prior verifier-free approaches is their reliance on a unique reference answer string  $y^*$  (Zhou et al., 2025). In mathematical reasoning, valid solutions often manifest in diverse forms (e.g., “1.6” vs. “8/5”). Strictly penalizing a reasoning trace that converges to a valid variant simply because it differs from the canonical string introduces *false negative signals*, thereby stifling legitimate exploration.

To mitigate this, for the **MATH** dataset where answer heterogeneity is common, we construct a set of semantically equivalent solution variants  $\mathcal{Y}^* = \{y_1^*, y_2^*, \dots, y_M^*\}$ . Specifically, we employ **Qwen2.5-32B-Instruct** to perform offline augmentation, generating up to 5 valid variations for each ground truth. Accordingly, we reformulate the step-conditioned likelihood  $\ell_k$  to be **equivalence-aware**:

$$\ell_k = \max_{y \in \mathcal{Y}^*} \left( \frac{1}{|\mathcal{Y}|} \sum_{t=1}^{|\mathcal{Y}|} \log \pi_\theta(y_t \mid x, s_{1\dots k}, y_{<t}) \right) \quad (9)$$

By maximizing the likelihood over the set  $\mathcal{Y}^*$ , our reward mechanism becomes invariant to surface-form diversity, ensuring that the model is credited for capturing the *underlying semantic truth* rather than performing rigid string matching.

**Models.** We employ **Qwen2.5-Instruct-3B** (Qwen et al., 2025) for text-only tasks and **Qwen2.5-VL-Instruct-3B** (Bai et al., 2025) for multimodal tasks.

**Implementation & Hardware Protocol.** All experiments are implemented using PyTorch and DeepSpeed ZeRO-3 for memory optimization.

- **Infrastructure:** Training is conducted in a multi-node setting, utilizing **2 nodes with 2 GPUs each** (4 GPUs total). The hardware pool consists of **NVIDIA A100 (80GB)** and **NVIDIA H100 (80GB)** GPUs.
- **Fair Comparison:** To eliminate hardware-induced variance, we strictly enforce a **homogeneous hardware protocol**: all comparative experiments (e.g., Ours vs. GRPO) on a specific dataset are guaranteed to be executed on the exact same GPU type (e.g., all MATH runs on H100, all GSM8K runs on A100).
- **Training Config:** We use a group size of  $G = 4$  and train for 2 epochs. The max prompt/completion lengths are set to 1024/4096. We use a constant temperature of 1.0 during rollout to encourage exploration.

## 4.2. Main Results

### 4.2.1. TRAINING DYNAMICS

We first investigate the sample efficiency and learning dynamics of our framework during the initial optimization phase.

**Sample Efficiency and Training Stability.** Figure 2 visualizes the trajectory of Pass@1 accuracy over training steps. We observe distinct optimization behaviors driven by our continuous reward framework:

- **Accelerated Convergence (The Cold-Start Advantage):** On structured tasks (GSM8K, Super-CLEVR), MIG establishes a significant performance lead within the first 100 steps. Unlike the outcome-sparse GRPO baseline, which struggles to assign credit during early exploration, MIG’s step-wise signals act as dense navigational cues, effectively guiding the policy through complex reasoning paths. This is particularly evident in **Super-CLEVR**, where MIG reaches near-saturation (~95%) while the baseline is still in the initial climbing phase.
- **Resilience to Reward Collapse:** On high-variance benchmarks like **MATH** and **CMM-Math**, the GRPO baseline exhibits significant oscillation and instability. In contrast, our method maintains a smoother ascent and a higher average baseline. This suggests that the monotonic constraint in our HWM mechanism effectively filters out noise, preventing the “forgetting” phenomena often observed in outcome-only reinforcement learning.

### 4.2.2. EVALUATION ON TEXT & VISION

All evaluation inference runs were conducted on a NVIDIA A100 (80GB) GPU with a sampling temperature set to 0.6.

- **Performance on Textual Reasoning.** Table 1 highlights the efficacy of our method across standard and competition-level math benchmarks. **(1) Mitigating Reward Hacking (SCQ5K):** A critical failure mode of outcome supervision is observed on SCQ5K-EN, where GRPO underperforms the Base model (62.0% vs. 64.0%). This potentially indicates *reward hacking*, where the model overfits to answer formatting rather than logical deduction. Our method eliminates this pathology, strictly improving performance to 73.0% (+11.0%) by valuing the reasoning process itself.
- **Performance on Visual Reasoning.** As shown in Table 2, Our method demonstrates superior generalization in multi-modal contexts. **(1) Handling Long-Horizon Spatial Logic:** On tasks requiring multi-step visual tracking (Super-CLEVR, CoGenT), MIG

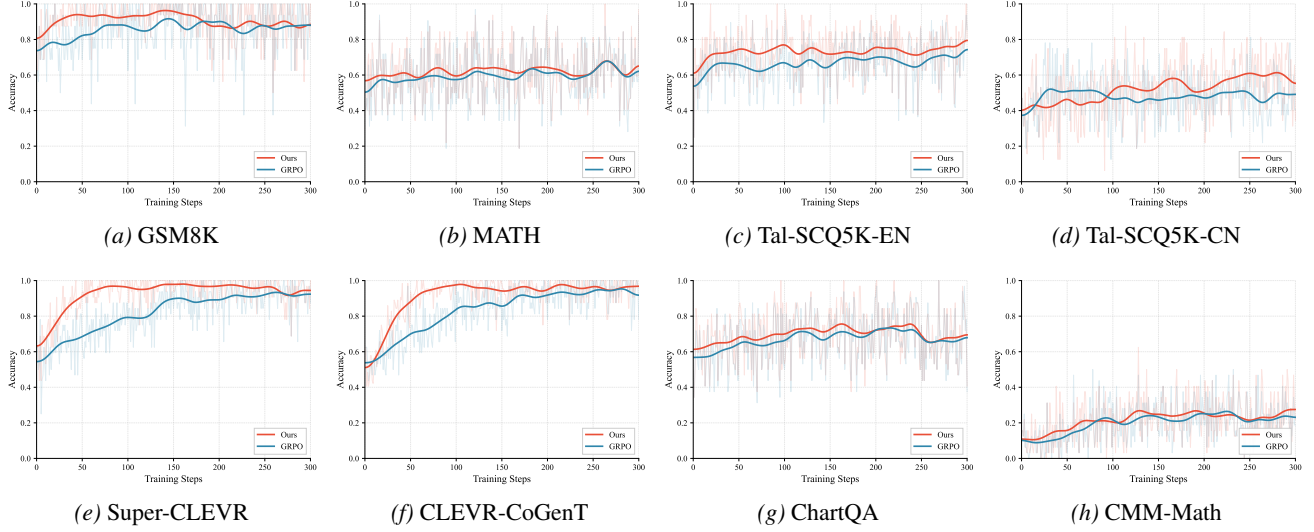


**Figure 2. Training Dynamics across Textual (Top) and Multimodal (Bottom) Benchmarks.** Plots show the training accuracy on rollout over steps. Faint lines indicate raw data, while solid lines denote Gaussian-smoothed trends. **Red curves (Ours)** consistently exhibit a steeper initial ascent compared to **GRPO (Blue)**, indicating superior sample efficiency. Notably, in structured reasoning tasks like GSM8K and Super-CLEVR, our Step-wise MIG reward enables the policy to discover valid reasoning paths significantly faster than the outcome-sparse baseline.

achieves dominant gains ( $>8.0\%$ ). By rewarding each correct step of spatial reasoning (e.g., intermediate object localization), MIG prevents the model from relying on spurious visual correlations. **(2) Overcoming Negative Transfer (MMStar):** OOD evaluation on MMStar reveals that GRPO suffers from *negative transfer* (dropping from 50.0% to 47.0%), implying it overfitted to the training distribution (ChartQA). Conversely, our method achieves positive transfer (+5.0%), proving that monotonic information gain fosters generalized reasoning capabilities that withstand distribution shifts.

## 5. Ablation Study

### The Role of Dual-Gated SFT

To validate the contribution of the *Dual-Gated SFT* objective, we trained a variant of our model (“Ours w/o SFT”) by setting the weight of SFT to zero, relying solely on the RL signals ( $\mathcal{L}_{\text{MIG}} + \mathcal{L}_{\text{Outcome}}$ ). We report the average accuracy across four diverse benchmarks: MATH (In-Domain), CommonsenseQA, SVAMP, and AIME 2025 (OOD).

**Results & Analysis.** Figure 3 illustrates the performance gap.

- **Marginal Gain on Standard Tasks:** On standard benchmarks like MATH and SVAMP, removing SFT leads to a relatively small performance drop (e.g., MATH: 61.4%  $\rightarrow$  60.8%). This suggests that for problems within the model’s comfort zone, the continuous MIG reward alone is sufficient to drive optimization.

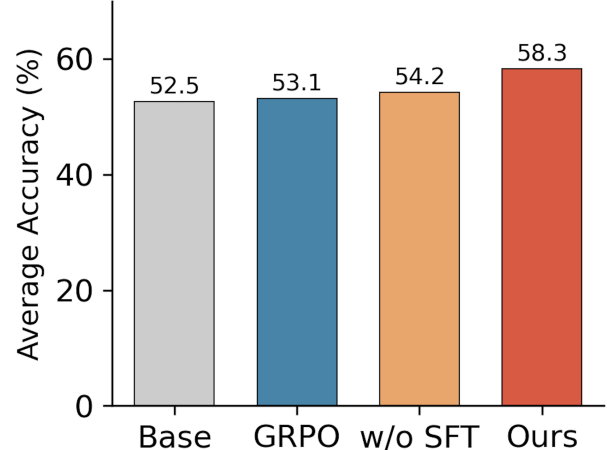


**Figure 3. Ablation Analysis on Average Performance.** We compare the average accuracy across four benchmarks (MATH, CSQA, SVAMP, AIME). While removing the SFT component (“w/o SFT”) causes only minor degradation on standard tasks, it leads to a catastrophic failure on the hardest benchmark (AIME), dropping the average performance significantly. This confirms that Dual-Gated SFT is essential for stabilizing complex reasoning capabilities.

**Table 1. Main Results on Text Reasoning Benchmarks.** We report **Pass@1** (Accuracy) and **Pass@8** (Potential). **Ours** consistently achieves the highest performance (**Bold**) across most metrics, while GRPO often ranks second (Underline) or lower. **In-Domain** tasks use task-specific training. **OOD** tasks evaluate the generalization of a single model trained on MATH (300 steps).

Dataset	Type	Base Model		GRPO		Ours		
		Pass@1	Pass@8	Pass@1	Pass@8	Pass@1	Pass@8	Δ Pass@1
<b>In-Domain Evaluation (Task-Specific Training)</b>								
GSM8K	Math	77.80	<u>93.20</u>	81.00	<b>95.60</b>	<b>83.20</b>	<b>95.60</b>	+2.20
Hendrycks MATH	Math	56.20	76.00	<u>58.00</u>	<u>80.20</u>	<b>61.40</b>	<b>81.00</b>	+3.40
TAL-SCQ5K (CN)	Science	49.00	77.00	<u>53.00</u>	85.00	<b>64.00</b>	<b>92.00</b>	+11.00
TAL-SCQ5K (EN)	Science	<u>64.00</u>	<u>86.00</u>	62.00	81.00	<b>73.00</b>	<b>90.00</b>	+11.00
<b>Out-of-Distribution (OOD) (Model transferred from MATH)</b>								
CommonsenseQA	Logic	69.00	<u>92.80</u>	69.40	92.80	<b>69.80</b>	<b>93.40</b>	+0.40
SVAMP	Robustness	<u>85.00</u>	<u>96.67</u>	85.00	<b>97.67</b>	<b>88.67</b>	<u>96.67</u>	+3.67
AIME 2025	Hard Math	<u>0.00</u>	<b>20.00</b>	<u>0.00</u>	13.33	<b>13.33</b>	<b>20.00</b>	+13.33

**Table 2. Main Results on Vision Reasoning Benchmarks.** We report **Pass@1** (Accuracy) and **Pass@8** (Potential). **MIG** demonstrates superior performance on In-Domain tasks (Super-CLEVR, CoGenT, ChartQA) and robust generalization on OOD tasks like MMStar. Note that for HallusionBench, while GRPO achieves higher Pass@1, MIG maintains significantly higher Pass@8 potential (97.0 vs 94.0), suggesting less overfitting. **OOD** models are transferred from ChartQA (300 steps).

Dataset	Type	Base Model		GRPO		Ours		
		Pass@1	Pass@8	Pass@1	Pass@8	Pass@1	Pass@8	Δ Pass@1
<b>In-Domain Evaluation (Task-Specific Training)</b>								
Super-CLEVR	3D Logic	46.00	80.00	<u>89.00</u>	<u>97.00</u>	<b>97.00</b>	<b>99.00</b>	+8.00
CoGenT	Compositionality	54.00	79.00	<u>82.00</u>	<u>95.00</u>	<b>91.00</b>	<b>98.00</b>	+9.00
ChartQA	Charts	79.00	<u>93.00</u>	<u>81.00</u>	<u>93.00</u>	<b>87.00</b>	<b>95.00</b>	+6.00
CMM-Math	Math	15.00	39.00	<u>30.00</u>	<b>57.00</b>	<b>36.00</b>	<u>54.00</u>	+6.00
<b>Out-of-Distribution (OOD) (Transfer from ChartQA)</b>								
MMStar	Multi-modal	<u>50.00</u>	<b>87.00</b>	47.00	<b>87.00</b>	<b>55.00</b>	<u>86.00</u>	+8.00
HallusionBench	Hallucination	69.00	<b>98.00</b>	<b>74.00</b>	94.00	<u>71.00</u>	<u>97.00</u>	-3.00
MathVista	Visual Math	<b>45.00</b>	<b>78.00</b>	<b>45.00</b>	<b>78.00</b>	<b>45.00</b>	71.00	0.00

- **Critical Stabilizer for Hard Reasoning:** The impact becomes stark on the extreme **AIME 2025** benchmark. While our full model achieves a breakthrough **13.3%**, the ablation model collapses back to **0.0%**, indistinguishable from the baseline. This indicates that while RL encourages exploration, the *Dual-Gated SFT* term is indispensable for consolidating rare, high-quality reasoning traces discovered during training. Without this stabilization, the model fails to retain the capability required for olympiad-level deduction.

More results and ablation study can be found in Appendix D.

## 6. Conclusion

In this work, we addressed the fundamental challenge of aligning Large Language Models (LLMs) with sparse outcome rewards. We introduced an efficient training framework that provides the continuous reward signal via **Step-wise Marginal Information Gain (MIG)**. By measuring

the semantic likelihood increment against a **Monotonic Historical Watermark**, our approach effectively assigns credit to pivotal reasoning steps while filtering out training noise.

Our extensive experimental evaluation yields three key take-aways:

1. **Efficiency via Step-wise Supervision:** Across eight diverse benchmarks, our method demonstrates significantly higher sample efficiency than traditional GRPO. The steeper learning curves on tasks like GSM8K and Super-CLEVR validate that intrinsic probabilistic rewards accelerate the discovery of optimal reasoning paths.
2. **Modality Agnosticism:** The consistent gains across both textual (MATH, SCQ5K) and multimodal (ChartQA, CMM-Math) domains prove that our step-wise likelihood mechanism is a universal proxy for logical progress, independent of the input modality.

3. **Robust Generalization:** Most notably, the method exhibits strong out-of-distribution robustness. While standard RL methods collapsed on the olympiad-level **AIME 2025** benchmark, highlighting its capacity to foster deep, transferable reasoning capabilities.

Future work will explore scaling our framework to larger base models. We believe that by extracting supervision directly from the model’s own probability landscape, our method offers a scalable and effective pathway for the next generation of reasoning alignment.

## References

Bai, S., Chen, K., Liu, X., Wang, J., Ge, W., Song, S., Dang, K., Wang, P., Wang, S., Tang, J., Zhong, H., Zhu, Y., Yang, M., Li, Z., Wan, J., Wang, P., Ding, W., Fu, Z., Xu, Y., Ye, J., Zhang, X., Xie, T., Cheng, Z., Zhang, H., Yang, Z., Xu, H., and Lin, J. Qwen2.5-VL Technical Report, February 2025. URL <http://arxiv.org/abs/2502.13923>.

Chen, C., Liu, Z., Du, C., Pang, T., Liu, Q., Sinha, A., Varakantham, P., and Lin, M. Bootstrapping Language Models with DPO Implicit Rewards, March 2025a. URL <http://arxiv.org/abs/2406.09760>.

Chen, H., Feng, Y., Liu, Z., Yao, W., Prabhakar, A., Heinecke, S., Ho, R., Mui, P., Savarese, S., Xiong, C., and Wang, H. Language Models are Hidden Reasoners: Unlocking Latent Reasoning Capabilities via Self-Rewarding, November 2024a. URL <http://arxiv.org/abs/2411.04282>.

Chen, L., Li, J., Dong, X., Zhang, P., Zang, Y., Chen, Z., Duan, H., Wang, J., Qiao, Y., Lin, D., et al. Are we on the right way for evaluating large vision-language models? *Advances in Neural Information Processing Systems*, 37: 27056–27087, 2024b.

Chen, L., Gao, H., Liu, T., Huang, Z., Sung, F., Zhou, X., Wu, Y., and Chang, B. G1: Bootstrapping Perception and Reasoning Abilities of Vision-Language Model via Reinforcement Learning, May 2025b. URL <http://arxiv.org/abs/2505.13426>.

Cobbe, K., Kosaraju, V., Bavarian, M., Chen, M., Jun, H., Kaiser, L., Plappert, M., Tworek, J., Hilton, J., Nakano, R., Hesse, C., and Schulman, J. Training Verifiers to Solve Math Word Problems, November 2021. URL <http://arxiv.org/abs/2110.14168>.

DeepSeek-AI, Guo, D., Yang, D., Zhang, H., Song, J., Zhang, R., Xu, R., Zhu, Q., Ma, S., Wang, P., Bi, X., Zhang, X., Yu, X., Wu, Y., Wu, Z. F., Gou, Z., Shao, Z., Li, Z., Gao, Z., Liu, A., Xue, B., Wang, B., Wu, B., Feng, B., Lu, C., Zhao, C., Deng, C., Zhang, C., Ruan, C., Dai, D., Chen, D., Ji, D., Li, E., Lin, F., Dai, F., Luo, F., Hao, G., Chen, G., Li, G., Zhang, H., Bao, H., Xu, H., Wang, H., Ding, H., Xin, H., Gao, H., Qu, H., Li, H., Guo, J., Li, J., Wang, J., Chen, J., Yuan, J., Qiu, J., Li, J., Cai, J. L., Ni, J., Liang, J., Chen, J., Dong, K., Hu, K., Gao, K., Guan, K., Huang, K., Yu, K., Wang, L., Zhang, L., Zhao, L., Wang, L., Zhang, L., Xu, L., Xia, L., Zhang, M., Zhang, M., Tang, M., Li, M., Wang, M., Li, M., Tian, N., Huang, P., Zhang, P., Wang, Q., Chen, Q., Du, Q., Ge, R., Zhang, R., Pan, R., Wang, R., Chen, R. J., Jin, R. L., Chen, R., Lu, S., Zhou, S., Chen, S., Ye, S., Wang, S., Yu, S., Zhou, S., Pan, S., Li, S. S., Zhou, S., Wu, S., Ye, S., Yun, T., Pei, T., Sun, T., Wang, T., Zeng, W., Zhao, W., Liu, W., Liang, W., Gao, W., Yu, W., Zhang, W., Xiao, W. L., An, W., Liu, X., Wang, X., Chen, X., Nie, X., Cheng, X., Liu, X., Xie, X., Liu, X., Yang, X., Li, X., Su, X., Lin, X., Li, X. Q., Jin, X., Shen, X., Chen, X., Sun, X., Wang, X., Song, X., Zhou, X., Wang, X., Shan, X., Li, Y. K., Wang, Y. Q., Wei, Y. X., Zhang, Y., Xu, Y., Li, Y., Zhao, Y., Sun, Y., Wang, Y., Yu, Y., Zhang, Y., Shi, Y., Xiong, Y., He, Y., Piao, Y., Wang, Y., Tan, Y., Ma, Y., Liu, Y., Guo, Y., Ou, Y., Wang, Y., Gong, Y., Zou, Y., He, Y., Xiong, Y., Luo, Y., You, Y., Liu, Y., Zhou, Y., Zhu, Y. X., Xu, Y., Huang, Y., Li, Y., Zheng, Y., Zhu, Y., Ma, Y., Tang, Y., Zha, Y., Yan, Y., Ren, Z. Z., Ren, Z., Sha, Z., Fu, Z., Xu, Z., Xie, Z., Zhang, Z., Hao, Z., Ma, Z., Yan, Z., Wu, Z., Gu, Z., Zhu, Z., Liu, Z., Li, Z., Xie, Z., Song, Z., Pan, Z., Huang, Z., Xu, Z., Zhang, Z., and Zhang, Z. DeepSeek-R1: Incentivizing Reasoning Capability in LLMs via Reinforcement Learning, January 2025. URL <http://arxiv.org/abs/2501.12948>.

Guan, T., Liu, F., Wu, X., Xian, R., Li, Z., Liu, X., Wang, X., Chen, L., Huang, F., Yacoob, Y., et al. Hallusionbench: an advanced diagnostic suite for entangled language hallucination and visual illusion in large vision-language models. In *Proceedings of the IEEE/CVF Conference on Computer Vision and Pattern Recognition*, pp. 14375–14385, 2024.

Gulcehre, C., Paine, T. L., Srinivasan, S., Konyushkova, K., Weerts, L., Sharma, A., Siddhant, A., Ahern, A., Wang, M., Gu, C., Macherey, W., Doucet, A., Firat, O., and Freitas, N. d. Reinforced Self-Training (ReST) for Language Modeling, August 2023. URL <http://arxiv.org/abs/2308.08998>.

Hendrycks, D., Burns, C., Kadavath, S., Arora, A., Basart, S., Tang, E., Song, D., and Steinhardt, J. Measuring Mathematical Problem Solving With the MATH Dataset, November 2021. URL <http://arxiv.org/abs/2103.03874>.

Li, Z., Tang, B., Niu, Y., Jin, B., Shi, Q., Feng, Y., Li, Z.,

Hu, J., Yang, M., and Xiong, F. CARE-STaR: Constraint-aware Self-taught Reasoner.

Li, Z., Wong, X., Stengel-Eskin, E., Kortylewski, A., Ma, W., Van Durme, B., and Yuille, A. Super-CLEVR: A Virtual Benchmark to Diagnose Domain Robustness in Visual Reasoning. In *2023 IEEE/CVF Conference on Computer Vision and Pattern Recognition (CVPR)*, pp. 14963–14973, Vancouver, BC, Canada, June 2023. IEEE. ISBN 979-8-3503-0129-8. doi: 10.1109/CVPR52729.2023.01437. URL <https://ieeexplore.ieee.org/document/10205295/>.

Liu, S.-Y., Dong, X., Lu, X., Diao, S., Belcak, P., Liu, M., Chen, M.-H., Yin, H., Wang, Y.-C. F., Cheng, K.-T., Choi, Y., Kautz, J., and Molchanov, P. GDPO: Group reward-Decoupled Normalization Policy Optimization for Multi-reward RL Optimization, January 2026. URL <http://arxiv.org/abs/2601.05242>.

Liu, T., Chen, Z., Fang, Z., Luo, W., Tian, M., and Liu, Z. MathEval: A Comprehensive Benchmark for Evaluating Large Language Models on Mathematical Reasoning Capabilities. *Frontiers of Digital Education*, 2(2):16, June 2025a. ISSN 2097-3918, 2097-3926. doi: 10.1007/s44366-025-0053-z. URL <https://link.springer.com/10.1007/s44366-025-0053-z>.

Liu, W., Pan, Q., Zhang, Y., Liu, Z., Wu, J., Zhou, J., Zhou, A., Chen, Q., Jiang, B., and He, L. CMM-Math: A Chinese Multimodal Math Dataset To Evaluate and Enhance the Mathematics Reasoning of Large Multimodal Models. In *Proceedings of the 33rd ACM International Conference on Multimedia*, pp. 12585–12591, Dublin Ireland, October 2025b. ACM. ISBN 979-8-4007-2035-2. doi: 10.1145/3746027.3758193. URL <https://dl.acm.org/doi/10.1145/3746027.3758193>.

Lu, P., Bansal, H., Xia, T., Liu, J., Li, C., Hajishirzi, H., Cheng, H., Chang, K.-W., Galley, M., and Gao, J. Mathvista: Evaluating mathematical reasoning of foundation models in visual contexts. *arXiv preprint arXiv:2310.02255*, 2023.

Masry, A., Long, D., Tan, J. Q., Joty, S., and Hoque, E. ChartQA: A Benchmark for Question Answering about Charts with Visual and Logical Reasoning. In *Findings of the Association for Computational Linguistics: ACL 2022*, pp. 2263–2279, Dublin, Ireland, 2022. Association for Computational Linguistics. doi: 10.18653/v1/2022.findings-acl.177. URL <https://aclanthology.org/2022.findings-acl.177>.

OpenAI, Jaech, A., Kalai, A., Lerer, A., Richardson, A., El-Kishky, A., Low, A., Helyar, A., Madry, A., Beutel, A., Carney, A., Iftimie, A., Karpenko, A., Passos, A. T., Neitz, A., Prokofiev, A., Wei, A., Tam, A., Bennett, A., Kumar, A., Saraiva, A., Vallone, A., Duberstein, A., Kondrich, A., Mishchenko, A., Applebaum, A., Jiang, A., Nair, A., Zoph, B., Ghorbani, B., Rossen, B., Sokolowsky, B., Barak, B., McGrew, B., Minaiev, B., Hao, B., Baker, B., Houghton, B., McKinzie, B., Eastman, B., Lugaresi, C., Bassin, C., Hudson, C., Li, C. M., Bourcy, C. d., Voss, C., Shen, C., Zhang, C., Koch, C., Orsinger, C., Hesse, C., Fischer, C., Chan, C., Roberts, D., Kappler, D., Levy, D., Selsam, D., Dohan, D., Farhi, D., Mely, D., Robinson, D., Tsipras, D., Li, D., Oprica, D., Freeman, E., Zhang, E., Wong, E., Proehl, E., Cheung, E., Mitchell, E., Wallace, E., Ritter, E., Mays, E., Wang, F., Such, F. P., Raso, F., Leoni, F., Tsimpourlas, F., Song, F., Lohmann, F. v., Sulit, F., Salmon, G., Parascandolo, G., Chabot, G., Zhao, G., Brockman, G., Leclerc, G., Salman, H., Bao, H., Sheng, H., Andrin, H., Bagherinezhad, H., Ren, H., Lightman, H., Chung, H. W., Kivlichan, I., O’Connell, I., Osband, I., Gilaberte, I. C., Akkaya, I., Kostrikov, I., Sutskever, I., Kofman, I., Pachocki, J., Lennon, J., Wei, J., Harb, J., Twore, J., Feng, J., Yu, J., Weng, J., Tang, J., Yu, J., Candela, J. Q., Palermo, J., Parish, J., Heidecke, J., Hallman, J., Rizzo, J., Gordon, J., Uesato, J., Ward, J., Huizinga, J., Wang, J., Chen, K., Xiao, K., Singhal, K., Nguyen, K., Cobbe, K., Shi, K., Wood, K., Rimbach, K., Gu-Lemberg, K., Liu, K., Lu, K., Stone, K., Yu, K., Ahmad, L., Yang, L., Liu, L., Maksin, L., Ho, L., Fedus, L., Weng, L., Li, L., McCallum, L., Held, L., Kuhn, L., Kondraciuk, L., Kaiser, L., Metz, L., Boyd, M., Trebacz, M., Joglekar, M., Chen, M., Tintor, M., Meyer, M., Jones, M., Kaufer, M., Schwarzer, M., Shah, M., Yatbaz, M., Guan, M. Y., Xu, M., Yan, M., Glaese, M., Chen, M., Lampe, M., Malek, M., Wang, M., Fradin, M., McClay, M., Pavlov, M., Wang, M., Wang, M., Murrati, M., Bavarian, M., Rohaninejad, M., McAleese, N., Chowdhury, N., Chowdhury, N., Ryder, N., Tezak, N., Brown, N., Nachum, O., Boiko, O., Murk, O., Watkins, O., Chao, P., Ashbourne, P., Izmailov, P., Zhokhov, P., Dias, R., Arora, R., Lin, R., Lopes, R. G., Gaon, R., Miyara, R., Leike, R., Hwang, R., Garg, R., Brown, R., James, R., Shu, R., Cheu, R., Greene, R., Jain, S., Altman, S., Toizer, S., Toyer, S., Miserendino, S., Agarwal, S., Hernandez, S., Baker, S., McKinney, S., Yan, S., Zhao, S., Hu, S., Santurkar, S., Chaudhuri, S. R., Zhang, S., Fu, S., Papay, S., Lin, S., Balaji, S., Sanjeev, S., Sidor, S., Broda, T., Clark, A., Wang, T., Gordon, T., Sanders, T., Patwardhan, T., Sottiaux, T., Degry, T., Dimson, T., Zheng, T., Garipov, T., Stasi, T., Bansal, T., Creech, T., Peterson, T., Eloundou, T., Qi, V., Kosaraju, V., Monaco, V., Pong, V., Fomenko, V., Zheng, W., Zhou, W., McCabe, W., Zaremba, W., Dubois, Y., Lu, Y., Chen, Y., Cha, Y., Bai, Y., He, Y., Zhang, Y., Wang, Y., Shao, Z., and Li, Z. OpenAI o1 System Card, December 2024. URL <http://arxiv.org/abs/2412.16720>.

Patel, A., Bhattacharya, S., and Goyal, N. Are nlp models really able to solve simple math word problems? *arXiv preprint arXiv:2103.07191*, 2021.

Qwen, Yang, A., Yang, B., Zhang, B., Hui, B., Zheng, B., Yu, B., Li, C., Liu, D., Huang, F., Wei, H., Lin, H., Yang, J., Tu, J., Zhang, J., Yang, J., Yang, J., Zhou, J., Lin, J., Dang, K., Lu, K., Bao, K., Yang, K., Yu, L., Li, M., Xue, M., Zhang, P., Zhu, Q., Men, R., Lin, R., Li, T., Tang, T., Xia, T., Ren, X., Ren, X., Fan, Y., Su, Y., Zhang, Y., Wan, Y., Liu, Y., Cui, Z., Zhang, Z., and Qiu, Z. Qwen2.5 Technical Report, January 2025. URL <http://arxiv.org/abs/2412.15115>.

Sahoo, S. The Good, The Bad, and The Hybrid: A Reward Structure Showdown in Reasoning Models Training, November 2025. URL <http://arxiv.org/abs/2511.13016>.

Shao, Z., Wang, P., Zhu, Q., Xu, R., Song, J., Bi, X., Zhang, H., Zhang, M., Li, Y. K., Wu, Y., and Guo, D. DeepSeekMath: Pushing the Limits of Mathematical Reasoning in Open Language Models, April 2024. URL <http://arxiv.org/abs/2402.03300>.

Su, M., Guan, J., Gu, Y., Huang, M., and Wang, H. Trust-Region Adaptive Policy Optimization, December 2025. URL <http://arxiv.org/abs/2512.17636>.

Talmor, A., Herzig, J., Lourie, N., and Berant, J. Commonsenseqa: A question answering challenge targeting commonsense knowledge. In *Proceedings of the 2019 Conference of the North American Chapter of the Association for Computational Linguistics: Human Language Technologies, Volume 1 (Long and Short Papers)*, pp. 4149–4158, 2019.

Tang, Y., Wang, S., Madaan, L., and Munos, R. Beyond Verifiable Rewards: Scaling Reinforcement Learning for Language Models to Unverifiable Data, May 2025. URL <http://arxiv.org/abs/2503.19618>.

Team, K., Bai, Y., Bao, Y., Chen, G., Chen, J., Chen, N., Chen, R., Chen, Y., Chen, Y., Chen, Y., Chen, Z., Cui, J., Ding, H., Dong, M., Du, A., Du, C., Du, D., Du, Y., Fan, Y., Feng, Y., Fu, K., Gao, B., Gao, H., Gao, P., Gao, T., Gu, X., Guan, L., Guo, H., Guo, J., Hu, H., Hao, X., He, T., He, W., He, W., Hong, C., Hu, Y., Hu, Z., Huang, W., Huang, Z., Huang, Z., Jiang, T., Jiang, Z., Jin, X., Kang, Y., Lai, G., Li, C., Li, F., Li, H., Li, M., Li, W., Li, Y., Li, Y., Li, Z., Li, Z., Lin, H., Lin, X., Lin, Z., Liu, C., Liu, C., Liu, H., Liu, J., Liu, J., Liu, L., Liu, S., Liu, T. Y., Liu, T., Liu, W., Liu, Y., Liu, Y., Liu, Y., Liu, Y., Liu, Z., Lu, E., Lu, L., Ma, S., Ma, X., Ma, Y., Mao, S., Mei, J., Men, X., Miao, Y., Pan, S., Peng, Y., Qin, R., Qu, B., Shang, Z., Shi, L., Shi, S., Song, F., Su, J., Su, Z., Sun, X., Sung, F., Tang, H., Tao, J., Teng, Q., Wang, C., Wang, D., Wang, F., Wang, H., Wang, J., Wang, J., Wang, J., Wang, S., Wang, S., Wang, Y., Wang, Y., Wang, Y., Wang, Y., Wang, Z., Wang, Z., Wang, Z., Wei, C., Wei, Q., Wu, W., Wu, X., Wu, Y., Xiao, C., Xie, X., Xiong, W., Xu, B., Xu, J., Xu, J., Xu, L. H., Xu, L., Xu, S., Xu, W., Xu, X., Xu, Y., Xu, Z., Yan, J., Yan, Y., Yang, X., Yang, Y., Yang, Z., Yang, Z., Yang, Z., Yao, H., Yao, X., Ye, W., Ye, Z., Yin, B., Yu, L., Yuan, E., Yuan, H., Yuan, M., Zhan, H., Zhang, D., Zhang, H., Zhang, W., Zhang, X., Zhang, Y., Zhao, H., Zhao, Y., Zheng, H., Zheng, S., Zhou, J., Zhou, X., Zhou, Z., Zhu, Z., Zhuang, W., and Zu, X. Kimi K2: Open Agentic Intelligence, July 2025. URL <http://arxiv.org/abs/2507.20534>.

Wu, S., Xie, J., Zhang, Y., Chen, A., Zhang, K., Su, Y., and Xiao, Y. ARM: Adaptive Reasoning Model, October 2025. URL <http://arxiv.org/abs/2505.20258>.

Yu, Q., Zhang, Z., Zhu, R., Yuan, Y., Zuo, X., Yue, Y., Dai, W., Fan, T., Liu, G., Liu, L., Liu, X., Lin, H., Lin, Z., Ma, B., Sheng, G., Tong, Y., Zhang, C., Zhang, M., Zhang, W., Zhu, H., Zhu, J., Chen, J., Chen, J., Wang, C., Yu, H., Song, Y., Wei, X., Zhou, H., Liu, J., Ma, W.-Y., Zhang, Y.-Q., Yan, L., Qiao, M., Wu, Y., and Wang, M. DAPO: An Open-Source LLM Reinforcement Learning System at Scale, May 2025. URL <http://arxiv.org/abs/2503.14476>.

Yuan, W., Pang, R. Y., Cho, K., Li, X., Sukhbaatar, S., Xu, J., and Weston, J. Self-Rewarding Language Models.

Yue, Y., Chen, Z., Lu, R., Zhao, A., Wang, Z., Yue, Y., Song, S., and Huang, G. Does Reinforcement Learning Really Incentivize Reasoning Capacity in LLMs Beyond the Base Model?, November 2025. URL <http://arxiv.org/abs/2504.13837>.

Zelikman, E., Wu, Y., Mu, J., and Goodman, N. D. STaR: Bootstrapping Reasoning With Reasoning, May 2022. URL <http://arxiv.org/abs/2203.14465>.

Zhang, D., Yu, Y., Dong, J., Li, C., Su, D., Chu, C., and Yu, D. MM-LLMs: Recent Advances in MultiModal Large Language Models, May 2024. URL <http://arxiv.org/abs/2401.13601>.

Zhang, J., Huang, J., Yao, H., Liu, S., Zhang, X., Lu, S., and Tao, D. R1-VL: Learning to Reason with Multi-modal Large Language Models via Step-wise Group Relative Policy Optimization, March 2025a. URL <http://arxiv.org/abs/2503.12937>.

Zhang, Z., Shan, Z., Song, K., Li, Y., and Ren, K. Linking Process to Outcome: Conditional Reward Modeling for LLM Reasoning, September 2025b. URL <http://arxiv.org/abs/2509.26578>.

Zhang, Z., Zheng, C., Wu, Y., Zhang, B., Lin, R., Yu, B.,  
Liu, D., Zhou, J., and Lin, J. The Lessons of Developing Process Reward Models in Mathematical Reasoning, June 2025c. URL <http://arxiv.org/abs/2501.07301>.

Zheng, C., Liu, S., Li, M., Chen, X.-H., Yu, B., Gao, C.,  
Dang, K., Liu, Y., Men, R., Yang, A., Zhou, J., and Lin, J. Group Sequence Policy Optimization, July 2025. URL <http://arxiv.org/abs/2507.18071>.

Zhou, X., Liu, Z., Sims, A., Wang, H., Pang, T., Li, C.,  
Wang, L., Lin, M., and Du, C. Reinforcing General Reasoning without Verifiers, May 2025. URL <http://arxiv.org/abs/2505.21493>.

## A. Prompt Template and Qualitative Examples

In this section, we provide the prompt template used for structured rollout and a qualitative example demonstrating our Step-Aware reasoning format.

### A.1. Instruction Prompt Template

We enforce a strict output format to facilitate step parsing. The system prompt provided to the policy model is shown below:

System Instruction & User Prompt
<p><b>User:</b>          Camden just bought 3/4 times as many dogs as Rico, who has 10 more dogs than Justin. If Justin has 14 dogs, what's the total number of legs that Camden's dogs have?</p> <p><b>System Constraints:</b>          You MUST follow this exact output format (no extra text):  <code>&lt;think&gt;</code>  <code>### Step 1</code>  <code>...</code>  <code>&lt;/think&gt;</code>  <code>&lt;answer&gt;FINAL_ANSWER_HERE&lt;/answer&gt;</code></p> <p><b>Strict Rules:</b></p> <ul style="list-style-type: none"> <li>• The final answer MUST appear ONLY inside <code>&lt;answer&gt;...&lt;/answer&gt;</code>.</li> <li>• The reasoning MUST be enclosed within <code>&lt;think&gt;...&lt;/think&gt;</code>.</li> <li>• Each step MUST start with: <code>"### Step X"</code> (X = 1, 2, 3, ...).</li> <li>• Ensure each step is a necessary logical link to reach the conclusion. Avoid meaningless repetition.</li> <li>• Do not add any headers or text outside the tags.</li> </ul>

### A.2. Model Trajectory Example

Below is a sample trajectory generated by model, demonstrating the step-wise breakdown parsed by our *Structured Rollout* phase.

Model Output
<p><code>&lt;think&gt;</code></p> <p><b>### Step 1</b>          First, let's determine how many dogs Rico has. According to the problem, Rico has 10 more dogs than Justin. Justin has 14 dogs. So, the number of dogs Rico has is: Rico's dogs = Justin's dogs + 10 = 14 + 10</p> <p><b>### Step 2</b>          Next, let's calculate the result from Step 1: Rico's dogs = 24</p> <p><b>### Step 3</b>          Now, we need to find how many dogs Camden has. Camden bought 3/4 times as many dogs as Rico. So, we multiply the number of dogs Rico has by 3/4:  <math>\text{Camden's dogs} = \frac{3}{4} \times \text{Rico's dogs}</math></p> <p><b>### Step 4</b>          Using the number of dogs Rico has from Step 2: Camden's dogs = <math>\frac{3}{4} \times 24</math></p> <p><b>### Step 5</b>          Let's calculate the result from Step 4: Camden's dogs = <math>(3 \times 24) \div 4 = 18</math></p> <p><b>### Step 6</b>          Camden's dogs are dogs, and each dog has 4 legs. Therefore, to find the total number of legs on Camden's dogs: Total</p>

number of legs = Number of dogs  $\times$  4

### ### Step 7

Finally, calculate the total number of legs: Total number of legs =  $18 \times 4$

### ### Step 8

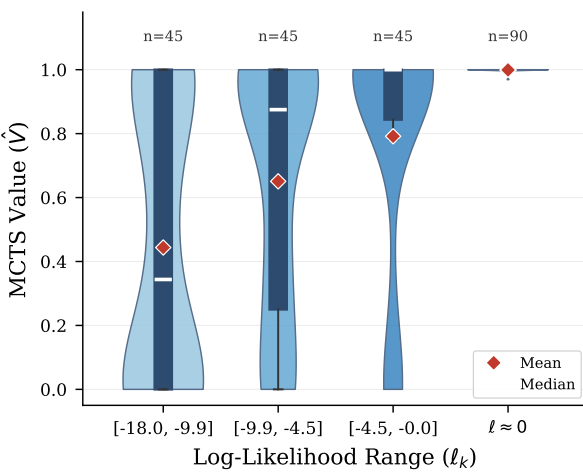
Let's perform the multiplication: Total number of legs =  $72 </\text{think}>$

`<answer>72</answer>`

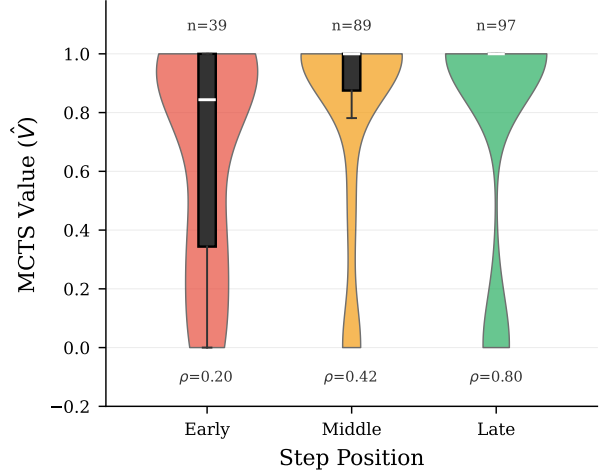
## B. Validation of the Step-Conditioned Likelihood Proxy

We empirically validate that our proposed step-conditioned average log-likelihood,  $\ell_k = \frac{1}{|y^*|} \sum_{t=1}^{|y^*|} \log \pi_\theta(y^* | x, s_1 \dots s_k, y_{<t}^*)$ , serves as a robust proxy for the true step value  $\hat{V}(s_k)$ .

**Data Collection Setup.** We sampled 100 problems from the GSM8K test set (Cobbe et al., 2021). To ensure meaningful step-wise analysis, we filtered out samples with fewer than 2 reasoning steps or parsing errors. This resulted in a curated dataset of 84 problems, yielding a total of 225 intermediate reasoning states. For each state  $s_k$ , we estimated its "true" value  $\hat{V}(s_k)$  via Monte Carlo Tree Search (MCTS) with 32 rollouts at temperature 0.6, defining the value as the fraction of rollouts that reached the correct answer. 3



(a) Value Distribution vs.  $\ell_k$



(b) Value Distribution vs. Step Position

**Figure 4. Empirical Validation of the Reward Proxy.** (a) Violin plots showing the distribution of MCTS-estimated values  $\hat{V}$  across different log-likelihood buckets. We observe a strong monotonic correlation: as  $\ell_k$  approaches 0 (higher confidence), both the median (white bar) and mean (red diamond) value increase sharply, confirming  $\ell_k$  as a reliable dense signal. (b) Value distribution across reasoning stages. While late steps generally exhibit higher values, early steps show significant variance with a "long tail" of high-value states.

**Visual Analysis.** Figure 4 provides visual confirmation of our hypothesis:

- **Likelihood as a Value Proxy (Fig. 4a):** There is a clear, non-linear monotonic relationship between our metric  $\ell_k$  and the ground truth value. Notably, states with  $\ell_k \approx 0$  almost universally correspond to terminal states with  $\hat{V} \approx 1.0$ , while lower likelihoods effectively separate low-quality states from promising ones.
- **The Pitfall of Position Bias (Fig. 4b):** While the correlation between step position and value increases from Early ( $\rho = 0.20$ ) to Late ( $\rho = 0.80$ ), the *Early* stage exhibits a wide bimodal distribution. A significant portion of early steps already possess high value (the upper bulb of the violin). Our content-aware  $\ell_k$  avoids this pitfall.

**Baseline Metrics.** We compared our metric ( $\ell_k$ ) against several baselines:

- **Likelihood Increment ( $\ell_k - \ell_0$ ):** The raw gain over the baseline without monotonic rectification.

- **Relative Position ( $k/T$ ):** A heuristic assuming linear progress over time.
- **Is last step:** Assuming only the last step matters.
- **Token Count:** Assuming longer reasoning implies better performance.
- **Random:** A sanity check baseline.

**Quantitative Results.** Table 3 presents the correlation analysis. We evaluated the alignment using Spearman’s rank correlation coefficient ( $\rho$ ) and the Area Under the ROC Curve (ROC-AUC), treating states with  $\hat{V}(s_k) > 0.5$  as positive samples.

*Table 3. Quantitative Comparison of Reward Proxies.* We evaluate alignment with MCTS-estimated ground truth values across 225 intermediate states from GSM8K.

Metric	Spearman $\rho$	ROC-AUC	p-value
$\ell_k$ (Ours)	<b>0.623</b>	0.844	$< 10^{-25}$
$\ell_k - \ell_0$	0.609	<b>0.846</b>	$< 10^{-24}$
Relative Position ( $k/T$ )	0.254	0.559	$1.2 \times 10^{-4}$
Is Last Step	0.176	0.526	$8.3 \times 10^{-3}$
Token Count	0.108	0.480	0.11
Random	0.026	0.507	0.70

**Analysis & Discussion.** As shown in Table 3, our proposed metric  $\ell_k$  achieves the highest correlation ( $\rho = 0.623$ ) with the ground truth value, demonstrating strong predictive power for logical correctness.

### B.1. Ablation Study on Reward Aggregation Strategies

Having established that the step-conditioned likelihood  $\ell_k$  is a valid proxy for value, a critical question remains: **How should we aggregate these dense signals into a final scalar reward  $R$  for policy optimization?**

We evaluated seven different aggregation strategies to transform the vector  $\ell = (\ell_1, \dots, \ell_K)$  into a scalar reward. We categorize these strategies into *Trajectory-level* (sparse) and *Step-level* (dense) methods. We computed the Spearman correlation ( $\rho$ ) and ROC-AUC of each aggregated reward against the MCTS-estimated ground truth value.

#### Baselines Compared.

1. **Final  $\ell_T$ :**  $R = \ell_T$ . Uses only the likelihood of the final state.
2. **Delta Sum ( $\ell_T - \ell_0$ ):**  $R = \ell_T - \ell_0$ . Equivalent to the sum of all increments.
3. **Mean  $\ell$ :**  $R = \frac{1}{T} \sum \ell_k$ . Simple average of confidence.
4. **Sum  $\ell$ :**  $R = \sum \ell_k$ . Accumulation of raw likelihoods.
5. **Position-Weighted Mean (PWM):**  $R = \frac{1}{T} \sum \ell_k \cdot \frac{k}{T}$ . Assigns higher weight to later steps.
6. **Clipped Delta:**  $R = \sum \text{clip}(\ell_k - \ell_{k-1}, -0.1, \infty)$ . Penalties for regression are capped.
7. **HWM (Ours):**  $R = \sum_{k=1}^T \max(0, \ell_k - h_{k-1})$ . Accumulates only "breakthroughs" above the historical maximum  $h_{k-1}$ .

**Results & Analysis.** Table 4 summarizes the performance of these strategies.

#### Observations:

- **The Trade-off between Correlation and Granularity:** As expected, *Final  $\ell_T$*  achieves the highest correlation ( $\rho = 0.827$ ) because the final state encapsulates the entire reasoning history. However, it discards all intermediate structural information, rendering it useless for **credit assignment** (identifying *which* step caused the error).

**Table 4. Comparison of Reward Aggregation Strategies.** We report the correlation with MCTS ground-truth values. While trajectory-level metrics (top) show high correlation, they fail to provide intermediate credit assignment. Among **step-level** methods, our **HWM** achieves the highest alignment with the true value function, significantly outperforming position-based and averaging heuristics.

Granularity	Aggregation Method	Spearman $\rho$	ROC-AUC	p-value
<i>Trajectory-level</i>	Final $\ell_T$	0.827	0.999	$3.1 \times 10^{-22}$
	Delta Sum ( $\ell_T - \ell_0$ )	0.670	0.982	$3.1 \times 10^{-12}$
<i>Step-level</i>	<b>HWM (Ours)</b>	<b>0.671</b>	<b>0.982</b>	$2.9 \times 10^{-12}$
	PWM (Position-Weighted)	0.623	0.949	$2.5 \times 10^{-10}$
	Mean $\ell$	0.600	0.932	$1.6 \times 10^{-09}$
	Sum $\ell$	0.573	0.912	$1.2 \times 10^{-08}$
	Clipped Delta	0.411	0.799	$1.0 \times 10^{-04}$

- **Superiority of HWM:** Among all dense reward methods, our **HWM** achieves the highest correlation ( $\rho = 0.671$ ). Notably, it matches the performance of the *Delta Sum* ( $\rho = 0.670$ ) but distributes the reward signal across specific breakthrough steps rather than collapsing it into a single scalar. This confirms that rewarding **non-monotonic breakthroughs** is the most effective way to densify the sparse signal.
- **Content  $\downarrow$  Position:** The **PWM** strategy, which mimics time-dependent weighting (e.g., linear ramp-up), underperforms HWM ( $\rho = 0.623$  vs 0.671). This empirically refutes the assumption that later steps are inherently more valuable. HWM succeeds by acknowledging that pivotal insights can occur at *any* stage, whereas PWM arbitrarily suppresses early logic.
- **Noise Filtering:** Simple averaging (*Mean  $\ell$* ) and accumulation (*Sum  $\ell$* ) perform worse, likely because they are sensitive to low-confidence oscillations in the reasoning chain. HWM’s  $\max(0, \cdot)$  mechanism effectively acts as a ReLU gate, filtering out these noisy fluctuations.

## C. Implementation Algorithm

Algorithm 1 presents a detailed summary of the complete training procedure of our framework.

---

### Algorithm 1 Step-wise MIG Policy Optimization

---

**Input:** Dataset  $\mathcal{D}$ , Solution Variants  $\mathcal{Y}^*$ , Policy  $\pi_\theta$ , Reference  $\pi_{\text{ref}}$ , Group Size  $G$

**Hyperparams:** SFT weight  $\alpha$ , Binary weight  $\gamma$ , Learning rate  $\eta$

**repeat**

    Sample a batch of prompts  $x$  from  $\mathcal{D}$

    /\* **Phase 1: Structured Rollout \*/**

        Sample group  $\{z^{(1)}, \dots, z^{(G)}\} \sim \pi_\theta(\cdot|x)$

        Parse each  $z^{(i)}$  into steps  $(s_1, \dots, s_K)$  and answer  $y^{(i)}$

    /\* **Phase 2: Step-Aware Valuation \*/**

**for**  $i = 1$  **to**  $G$  **do**

        Compute baseline  $\ell_0 \leftarrow \max_{y \in \mathcal{Y}^*} \log \pi(y|x)$

        Initialize HWM  $h_0 \leftarrow \ell_0$  and cumulative reward  $R_{\text{MIG}}^{(i)} \leftarrow 0$

**for**  $k = 1$  **to**  $K$  **do**

            // **Step-wise Likelihood**

$\ell_k \leftarrow \max_{y \in \mathcal{Y}^*} \frac{1}{|y|} \sum \log \pi_\theta(y|x, s_{1:k})$

            // **Monotonic Historical Watermark Update**

$h_k \leftarrow \max(h_{k-1}, \ell_k)$

            // **Rectified Breakthrough Gain**

$g_k \leftarrow \max(0, \ell_k - h_{k-1})$

$R_{\text{MIG}}^{(i)} \leftarrow R_{\text{MIG}}^{(i)} + g_k$

**end for**

        // **Outcome & Format Valuation**

        Compute correctness  $r_{\text{acc}}^{(i)} \in \{0, 1\}$  and format score  $r_{\text{fmt}}^{(i)} \in \{0, 1\}$

$R_{\text{out}}^{(i)} \leftarrow r_{\text{fmt}}^{(i)} + \gamma \cdot r_{\text{acc}}^{(i)}$

        Set SFT gates:  $\omega_{\text{struct}}^{(i)} \leftarrow r_{\text{fmt}}^{(i)}$ ,  $\omega_{\text{acc}}^{(i)} \leftarrow r_{\text{acc}}^{(i)}$

**end for**

    /\* **Phase 3: Hybrid Optimization \*/**

    Compute Advantages:

$A^{\text{step}} \leftarrow \text{GroupNorm}(\{R_{\text{MIG}}^{(1)}, \dots, R_{\text{MIG}}^{(G)}\})$

$A^{\text{out}} \leftarrow \text{GroupNorm}(\{R_{\text{out}}^{(1)}, \dots, R_{\text{out}}^{(G)}\})$

    Compute Decoupled Losses:

$\mathcal{L}_{\text{MIG}} \leftarrow -\frac{1}{G} \sum_i \sum_{t \in M_{\text{cot}}} \frac{\pi_\theta(t)}{\pi_{\text{ref}}(t)} A_i^{\text{step}}$

$\mathcal{L}_{\text{Outcome}} \leftarrow -\frac{1}{G} \sum_i \sum_{t \in M_{\text{comp}}} \frac{\pi_\theta(t)}{\pi_{\text{ref}}(t)} A_i^{\text{out}}$

$\mathcal{L}_{\text{SFT}} \leftarrow -\frac{1}{G} \sum_i (\omega_{\text{struct}}^{(i)} \cdot \omega_{\text{acc}}^{(i)}) \log \pi_\theta(z^{(i)}, y^{(i)}|x)$

$\mathcal{L}_{\text{Total}} \leftarrow \mathcal{L}_{\text{MIG}} + \mathcal{L}_{\text{Outcome}} + \alpha \mathcal{L}_{\text{SFT}}$

        Update  $\theta \leftarrow \theta - \eta \nabla \mathcal{L}_{\text{Total}}$

**until** Convergence

---

## D. More results

### D.1. Ablation Study: The Role of Gated-SFT Across Difficulty Levels

To decouple the effects of supervised guidance from reinforcement learning, we analyze the performance breakdown across the five difficulty levels of the Hendrycks MATH dataset (Table 5).

**SFT Prevents Foundational Collapse (Level 1).** A critical observation is the behavior on the easiest problems (Level 1). The outcome-based baseline (GRPO) suffers from severe *reward hacking*, where the policy degrades significantly compared to the Base model (81.4%  $\rightarrow$  74.4%) in pursuit of maximizing rewards on harder samples. Our ablated model  $\text{MIG}_{\text{w/o SFT}}$  partially mitigates this but still underperforms the Base model (79.1%). However, the full **MIG** framework, which integrates Gated-SFT, not only recovers this loss but achieves a dominant **86.0%** accuracy. This confirms that the SFT component acts as a stabilizer, preserving and refining the model’s foundational capabilities.

**Step-wise RL Drives Deep Reasoning (Level 5).** On the hardest problems (Level 5), the story flips. The ablated  $\text{MIG}_{\text{w/o SFT}}$  model achieves the highest performance (**35.1%**), outperforming both GRPO (33.6%) and the Full MIG model (33.6%). This result is profound: it suggests that on extremely complex tasks, human-annotated traces (SFT) might act as a “ceiling” or introduce bias that limits exploration. The pure Step-wise MIG reward allows the model to discover novel, more effective reasoning paths.

**Conclusion.** Our Hybrid Optimization strategy (Full MIG) represents a deliberate trade-off. By sacrificing a marginal amount of peak performance on Level 5 (35.1%  $\rightarrow$  33.6%), we secure a massive gain in foundational reliability on Level 1 (79.1%  $\rightarrow$  86.0%), resulting in the highest overall average (61.4%).

**Table 5. Performance Breakdown by Difficulty Level on Hendrycks MATH.** We compare the Base model, GRPO, our full method, and the ablated version without Gated-SFT (Ours<sub>w/o SFT</sub>). **Analysis:** (1) On **Level 1**, GRPO suffers from catastrophic forgetting (74.4% vs Base 81.4%), while our Full method utilizes SFT to achieve state-of-the-art results (86.0%). (2) On **Level 5**, the ablated  $\text{MIG}_{\text{w/o SFT}}$  achieves the highest accuracy (35.1%), suggesting that step-wise rewards alone drive deeper reasoning, though the combination (Full MIG) offers the best overall trade-off.

Method	Level 1	Level 2	Level 3	Level 4	Level 5	Avg.
Base Model	81.4	76.7	64.8	57.0	26.9	56.2
GRPO (Baseline)	74.4	75.6	71.4	54.7	33.6	58.0
Ours <sub>w/o SFT</sub> (Ablation)	79.1	<b>78.9</b>	<b>77.1</b>	55.5	<b>35.1</b>	60.8
<b>Ours (Full)</b>	<b>86.0</b>	77.8	<b>77.1</b>	<b>57.8</b>	33.6	<b>61.4</b>

### D.2. Ablation Study: Breakdown by Problem Type on SVAMP (OOD)

To further investigate how our method generalizes to out-of-distribution arithmetic variations, we categorize the SVAMP dataset by problem type (Table 6). This breakdown reveals a distinct functional separation between the SFT and RL components of our loss function.

**Procedural vs. Abstract Reasoning.** The results on SVAMP mirror the findings from the MATH difficulty ablation, providing a complementary perspective:

- **Procedural Mastery (Multiplication/Addition):** On tasks requiring strict adherence to algorithmic procedures, such as **Multiplication**, the combination of SFT and RL (Full MIG) yields massive gains compared to the ablated version (90.9% vs. 78.8%). This confirms that Gated-SFT is essential for stabilizing complex calculation routines.
- **Abstract Logic (Common-Divisor):** Conversely, on **Common-Divisor** problems involving number theory concepts, the ablated Ours<sub>w/o SFT</sub> outperforms all other methods, including the Full method (83.3% vs. 77.1%). This suggests that SFT data might introduce human biases or formatting constraints that are suboptimal for this specific reasoning type. Pure step-wise exploration allows the model to discover more robust logical paths for abstract number properties, unhindered by supervised imitation.

**Table 6. Performance Breakdown by Problem Type on SVAMP.** We compare the Base model, GRPO, Our method, and the ablated Ours<sub>w/o</sub> SFT. Our full method dominates on procedural tasks (Multiplication/Addition) where standard algorithms apply. However, on **Common-Divisor** problems, which require deeper number-theoretic insight, the ablated Ours<sub>w/o</sub> SFT achieves the best performance (83.3%), suggesting that SFT priors may sometimes constrain reasoning in abstract logical domains.

Method	Subtraction	Common-Divisor	Multiplication	Addition
Base Model	88.8	79.2	75.8	84.7
GRPO (Baseline)	88.8	75.0	78.8	86.4
Ours <sub>w/o</sub> SFT (Ablation)	87.5	<b>83.3</b>	78.8	89.8
<b>Ours (Full)</b>	<b>90.6</b>	77.1	<b>90.9</b>	<b>91.5</b>

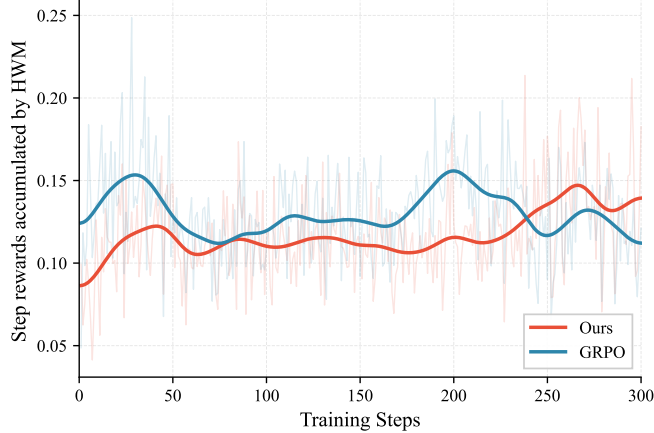


**Figure 5. Evolution of Accumulated Step-wise Rewards (HWM).** The curve illustrates the average accumulated monotonic information gain per episode during training. **MIG (Ours)** demonstrates a consistent upward trajectory, confirming that the model learns to generate strictly positive information increments throughout the reasoning chain. In contrast, the outcome-based **GRPO** baseline fails to accumulate intermediate dense rewards, highlighting the sparsity of its supervision signal.

### D.3. Validation of Monotonic Accumulation.

To verify that our framework essentially densifies the supervision signal, we visualize the evolution of accumulated step-wise rewards in Figure 5. The metric represents the cumulative Monotonic Information Gain ( $g_k$ ) defined by our HWM mechanism.

As hypothesized, **Ours** exhibits a steady ascent in accumulated rewards (Red curve), indicating that the model is continuously learning to produce intermediate “breakthrough” steps that exceed historical watermarks. This implies that the reasoning capability is being built layer-by-layer, step-by-step. Conversely, the **GRPO** baseline (Blue curve) remains near zero on this metric. Since GRPO optimizes solely for the final outcome, it lacks the incentive to maximize intermediate information density, confirming that outcome-based reinforcement leaves the internal reasoning structure largely unstructured and sparse.

### D.4. Qualitative Analysis and Failure Modes

To provide a deeper understanding of the behavioral differences between our Step-wise MIG framework and the traditional GRPO, we present two representative case studies. These examples illustrate both the capability of MIG in handling deep reasoning chains and the potential pitfalls of over-decomposition in simpler tasks.

#### D.4.1. CASE STUDY 1: DEEP REASONING CAPABILITY (LEVEL 5)

**Problem:** The proper divisors of 12 are 1, 2, 3, 4 and 6. A proper divisor of an integer  $N$  is a positive divisor of  $N$  that is less than  $N$ . What is the sum of the proper divisors of the sum of the proper divisors of 284?

**Correct Answer:** 284 (Note: 220 and 284 are an amicable pair).

Comparison on Multi-hop Reasoning

**MIG (Ours) - Correct ✓**

(Total 20 Steps, 941 Tokens)

**Step 1-8:** Identifies proper divisors of 284:  $\{1, 2, 4, 71, 142\}$ .

**Step 9-11:** Calculates sum:  $1 + 2 + 4 + 71 + 142 = 220$ .

**Step 12-15:** Crucial Transition. Now finds proper divisors of the intermediate result 220:  $\{1, 2, 4, 5, 10, 11, 20, 22, 44, 55, 110\}$ .

**Step 16-19:** Calculates second sum:  $1 + 2 + \dots + 110 = 284$ .  
**Step 20:** Final Answer: 284.

**Analysis:** The step-wise reward encourages the model to treat the second iteration (finding divisors of 220) as a new source of information gain. The reasoning chain is sustained until the full prompt requirement is met.

**GRPO (Baseline) - Incorrect ✗**

(Total 7 Steps, 666 Tokens)

**Step 1:** Identifies proper divisors of 284 correctly.

**Step 2:** Calculates sum: 220.

**Step 3:** Identifies proper divisors of 220.

**Step 4-5:** Computation Collapse. Instead of summing them, the model loses track of the nested objective.

**Step 6-7:** Prematurely concludes that the intermediate result (or a hallucinated sum) is the answer.

**Answer:** 220.

**Analysis:** GRPO suffers from *Goal Misalignment*. Without dense signals, the model stops after the first significant milestone (220), failing to execute the recursive logic required for the second layer.

D.4.2. CASE STUDY 2: THE COST OF GRANULARITY (LEVEL 3)

**Problem:** The area of triangle  $ABC$  is equal to  $a^2 - (b - c)^2$ . Compute  $\tan A$ .

**Correct Answer:** 8/15.

Comparison on Algebraic Manipulation

**MIG (Ours) - Incorrect ✗**

(Total 19 Steps, 1199 Tokens)

**Step 1-5:** Expands  $a^2 - (b - c)^2$  and equates to  $\frac{1}{2}bc \sin A$ . Correctly derives  $bc \sin A = 2bc(1 - \cos A)$ .

**Step 6-16:** Over-Decomposition. Breaks down the quadratic equation solving into minute arithmetic steps.

**Step 17:** Calculation Error. "Solving  $17x^2 - 32x + 15 = 0$ ..." In the explicit expansion of the quadratic formula, a sign error occurs due to the lengthy context.

**Step 18-19:** Propagates error to final result.

**Answer:** 4.

**Analysis:** Error Accumulation. While the logic is sound, the excessive granularity (19 steps for a standard algebra problem) increases the surface area for arithmetic hallucinations.

**GRPO (Baseline) - Correct ✓**

(Total 5 Steps, 1060 Tokens)

**Step 1-2:** Direct derivation using Cosine Rule. Arrives at  $\sin A = 4(1 - \cos A)$  quickly.

**Step 3-4:** Efficiently solves the quadratic equation for  $\cos A$ .

**Step 5:** Calculates  $\tan A = \frac{8/17}{15/17} = 8/15$ .

**Answer:** 8/15.

**Analysis:** For simpler procedural tasks, the baseline's concise path reduces the probability of calculation errors. This highlights a trade-off: dense rewards drive depth, but outcome rewards may favor efficiency in simpler domains.

**Summary of Qualitative Findings.** The comparison above highlights a fundamental trade-off in reasoning optimization:

- Deep Reasoning vs. Premature Stopping (Case 1):** On complex, recursive tasks (Level 5), outcome-only baselines like GRPO often suffer from *premature stopping*, where the model halts at an intermediate milestone (e.g., finding the first sum 220) because the final reward signal is too sparse to encourage further computation. MIG's step-wise incentives successfully drive the model to complete the full "multi-hop" reasoning chain.
- Granularity vs. Error Accumulation (Case 2):** Conversely, on standard procedural tasks (Level 3), MIG tends to generate longer, more granular chains (19 steps vs. 5 steps). While logically rigorous, this *over-decomposition* introduces more opportunities for arithmetic "hallucinations" or calculation errors ( $P(\text{fail}) \propto \text{Length}$ ). This suggests that future work could explore dynamic step-reward scaling, encouraging conciseness for simpler sub-tasks while reserving high granularity for complex logical leaps.